Available online at www.sciencedirect.com
ScienceDirect
Ceramics International 33 (2007) 1603–1610
CERAMICS INTERNATIONAL
www.elsevier.com/locate/ceramint

Densification and properties of zirconia prepared by three different sintering techniques

P. Dahl [a], I. Kaus [a], Z. Zhao [b], M. Johnsson [b], M. Nygren [b], K. Wiik [a], T. Grande [a], M.-A. Einarsrud [a,*]

[a] *Department of Materials Science and Engineering, Norwegian University of Science and Technology, N-7491 Trondheim, Norway*
[b] *Inorganic Chemistry, Arrhenius Laboratory, Stockholm University, SE-106 91 Stockholm, Sweden*

Received 6 June 2006; received in revised form 21 July 2006; accepted 22 July 2006
Available online 12 September 2006

Abstract

Densification of nanocrystalline yttria stabilized zirconia (YSZ) powder with 8 mol% Y_2O_3, prepared by a glycine/nitrate smoldering combustion method, was investigated by spark plasma sintering, hot pressing and conventional sintering. The spark plasma sintering technique was shown to be superior to the other methods giving dense materials (≥96%) with uniform morphology at lower temperatures and shorter sintering time. The grain size of the materials was 0.21, 0.37 and 12 μm after spark plasma sintering, hot pressing and conventional sintering, respectively. Total electrical conductivity of the materials showed no clear correlation with the grain size, but the activation energy for spark plasma sintered materials was slightly higher than for materials prepared by the two other densification methods. The hardness, measured by the Vickers indentation method, was found to be independent on grain size while fracture toughness, derived by the indentation method, was slightly decreasing with increasing grain size.

Keywords: B. Grain size; C. Electrical conductivity; C. Hardness; YSZ; Densification; Fracture toughness

1. Introduction

Yttria stabilized zirconia (YSZ) with its high ionic and low electronic conductivity is generally the material of choice as an electrolyte in solid oxide fuel cells (SOFC). In order to improve the conductivity and thereby lower the operating temperature alternative electrolyte materials (i.e. doped CeO_2) have been suggested but also often rejected due to poor mechanical properties. Improved conductivity in the traditional YSZ materials is therefore desired. Increasing conductivity with decreasing grain size has been reported for YSZ thin films [1,2] and nanocrystalline YSZ bulk materials may therefore give the desired improvement of the ionic conductivity. It is not given, however, that the properties observed for thin films can be directly converted into nanostructured bulk material properties. The reported changes in ionic conductivity for bulk YSZ with different grain size are small (or not existing) [3–8]. Factors such as density, sintering technique and effects due to impurities must be considered before concluding with an effect of grain size.

Thin films with grain size down to ~10 nm have been prepared [2]. The preparation of nanocrystalline bulk materials is more challenging since higher temperatures and longer sintering times compared to those for films are usually needed. The grain growth normally occurs during the final stage of the sintering process were the temperature is highest. In hot pressing (HP) and spark plasma sintering (SPS) uniaxial pressure is applied during sintering allowing densification at reduced temperature and time and thereby suppressing the grain growth. The SPS technique, where a pulsed direct current is passed through an electrical conducting pressing die working as the heating element gives more rapid densification rate due to the use of pressure and rapid heating rate. The presence of a pulsed electrical field that during the initial part of the sintering might create sparks that clean the particles surface and thus facilitate grain boundary diffusion and electrical field enhanced diffusion processes might also contribute to increased densification rate [9].

* Corresponding author.
E-mail address: Mari-Ann.Einarsrud@material.ntnu.no (M.A. Einarsrud).

0272-8842/$32.00
doi:10.1016/j.ceramint.2006.07.005

The objective of the present work is to evaluate different densification methods for the preparation of dense fine grained bulk YSZ materials. Moreover, possible effects of the grain size on the total conductivity and the mechanical properties of these materials are also explored.

2. Experimental

2.1. Sample preparation

Nanocrystalline YSZ powder (8 mol% Y_2O_3) was prepared as previously described using a glycine/nitrate smoldering combustion method [10]. Powder synthesized with the optimal glycine/nitrate ratio of 0.23 was calcined in oxygen flow at 650 °C for 24 h, ball milled for 12 h and dried at 400 °C for 12 h. This preparation method resulted in single phase powder with crystallite size less than 10 nm and a particle size less than 50 nm calculated from surface area [10]. A small amount of residual carbonate species was present in the powder after calcination [10]. The theoretical density calculated from the X-ray diffraction patterns was 5.96 g/cm^3 [10]. The powders were sieved (250 μm) before compacting and sintering.

Green bodies for conventional sintering were prepared by uniaxial pressing at 64 MPa followed by cold isostatic pressing (CIP) at 200 MPa giving green body density around 43% of theoretical density.

2.2. Densification

Dilatometry (Netzsch, DIL 402 C) on green body cylinders was performed in ambient air with a heating rate of 120 °C/h up to 1450 °C. For densification studies, three different sintering techniques were used; spark plasma sintering, hot pressing and conventional sintering. The SPS (Dr. Sinter 2050, Sumitomo Coal Mining Co. Ltd., Japan) was performed in vacuum using cylindrical graphite dies also working as the heating element. A uniaxial pressure varying from 50 to 110 MPa was applied at room temperature and released at the end of the holding time at the sintering temperature. The sintering temperature varied from 1100 to 1300 °C and the holding time varied from 0 to 10 min. A heating rate of 100 °C/min between 600 and 1300 °C and a cooling rate of >350 °C/min down to 1000 °C was used. Previous studies have shown that this is a reasonable cooling rate [11].

HP was performed under nitrogen flow in a clam furnace (Entech, VSTF 40/15) using cylindrical graphite dies with an inner diameter of 15 mm. No compaction of the starting powders was made prior to the sintering. After heating to 600 °C with a rate of 600 °C/h, a uniaxial pressure of 25 MPa was applied before heating to sintering temperature (1150–1300 °C) at a rate of 300 °C/h. The pressure was released after desired sintering time (varying from 0 to 6 h) at this temperature followed by a cooling to room temperature at 600 °C/h.

Conventional sintering was performed in air in a muffle furnace (Entech, SF-4/17). Green bodies were sintered at temperatures from (i) 1150 to 1300 °C for 1 h with a heating rate of 300 °C/h from 600 °C (cooling rate 600 °C/h) or (ii) 1500 °C for 12 h with a heating/cooling rate of 200 °C/h. Final density was measured by the Archimedean method (ISO 5017) in isopropanol.

2.3. Microstructure

The microstructure of the densified samples was studied by field emission scanning electron microscopy (FE-SEM) (Hitachi S-4300SE) on polished and thermally etched surfaces. Thermal etching for 12 min at a temperature 50 °C below sintering temperature was used. Average grain size was estimated from the FE-SEM micrographs using the linear intercept method [12]. For the specimens with average grain size above 1 μm the measurements were done over a minimum of 50 grains while a minimum of 100 grains were used for determining grain sizes below 1 μm.

2.4. Electrical conductivity

Electrical conductivity measurements were performed using the van der Pauw technique [13] on sintered, polished (parallel planar) specimens. With four platinum electrodes attached to the specimen surface close to the circumference, the samples were slowly heated (1 °C/min) to 1000 °C in a vertical tube furnace. At constant temperatures, from ∼1000 to ∼500 °C (and back up to ∼1000 °C), the specific electrical conductivity was calculated from perpendicular sets of currents (I_1, I_2) and voltages (U_1, U_2).

2.5. Mechanical properties

Hardness was calculated using the Vickers indentation method (Matsuzawa DVK-1S) [14] on polished surfaces. For each sample, 10–12 indents were made with an applied load of 2.9 N and measured by optical microscopy (Reickert MeF3 A) using a digital camera (Sony DXC-950P colour video camera). For fracture toughness (K_{IC}) calculations [14], 10 indents with an applied load of 49 N, were made for each sample. K_{IC} was derived from average crack length, measured by SEM (Hitachi S-3500N), as well as experimental Vickers hardness values and a modulus of elasticity (E = 218 GPa) previously reported by Donzel and Roberts [15].

3. Results

3.1. Densification

The curves in Fig. 1, derived from linear shrinkage, show how the density varied with time during SPS and conventional sintering. The sintering rate was higher for SPS as close to full density (>96%) was achieved within minutes whereas hours were needed in order to obtain dense materials by conventional sintering. Dense materials were achieved at significantly lower temperature by SPS (1150–1200 °C) compared to conventional sintering (1450 °C). Maximum sintering rate (derived from the slope of the curves) was found between 1100 and 1150 °C for

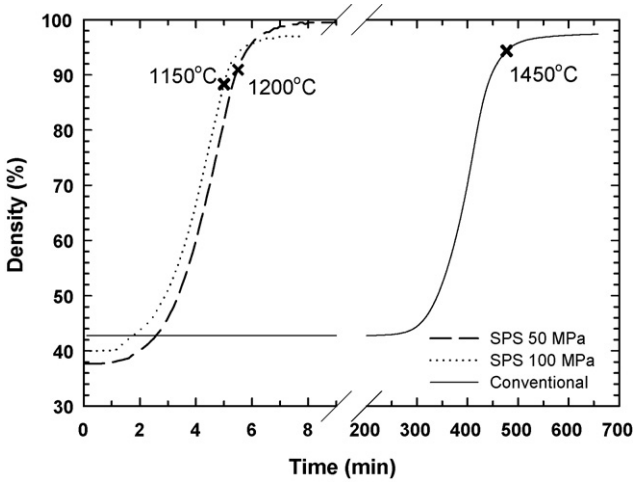

Fig. 1. Change in density of YSZ during SPS and conventional sintering as a function of sintering time. The markes (×) indicates time for which the isothermal sintering temperatures were obtained. Densities for SPS specimens are derived directly from linear shrinkage during sintering and the final density measured by the Archimedean method. Densities for conventional sintering are calculated using both green and final density with the linear shrinkage (dL/L_0) as a scaling factor.

SPS and about 1250 °C for the conventional sintering. As seen from Fig. 1 the densification started slightly earlier when the applied pressure during SPS was increased from 50 to 100 MPa however, the sintering rate was not affected.

The SPS and HP specimens were grey or black depending on sintering time. The colour changed to white upon heating to temperatures above ∼1000 °C in ambient air. Sintering conditions as well as final density of the sintered specimens are listed in Table 1. Each specimen is given a numerical ID indicating temperature–pressure–time. Final densities achieved by isothermal SPS, HP and conventional sintering are displayed in Fig. 2(a). SPS is superior as a relative density of 96.3% was obtained at 1150 °C (SPS-1150-70-5). Conventional sintering at equivalent temperatures gives significantly lower density than SPS and HP.

Table 1
Sintering parameters and densities of YSZ specimens obtained from different sintering techniques

Specimen ID	Temperature (°C)	Applied pressure (MPa)	Time	Density (%)
CS-1500-0-12	1500	–	12 h	97.4
HP-1200-25-1	1200	25	1 h	90.8
HP-1200-25-6	1200	25	6 h	93.6
HP-1250-25-0.5	1250	25	0.5 h	93.9
HP-1250-25-1	1250	25	1 h	96.9
HP-1250-25-3	1250	25	3 h	97.0
HP-1300-25-0	1300	25	0 h	92.3
HP-1300-25-0.5	1300	25	0.5 h	97.5
HP-1300-25-1	1300	25	1 h	99.3
SPS-1150-70-5	1150	70	5 min	96.3
SPS-1200-70-5	1200	70	5 min	97.3
SPS-1250-70-5	1250	70	5 min	98.4
SPS-1300-70-5	1300	70	5 min	98.5
SPS-1200-50-0	1200	50	0 min	85.8
SPS-1200-50-1	1200	50	1 min	94.0
SPS-1200-50-5	1200	50	5 min	98.8
SPS-1200-50-10	1200	50	10 min	99.5
SPS-1100-110-8	1100	110	8 min	96.0
SPS-1150-100-5	1150	100	5 min	96.3
SPS-1150-100-3*	1150	100[a]	3 min	98.5
SPS-1150-100-5*	1150	100[a]	5 min	99.3

CS, HP and SPS denote conventional sintering, hot pressing and spark plasma sintering, respectively. The number code indicates temperature–pressure–time.
[a] Pressure applied at sintering temperature.

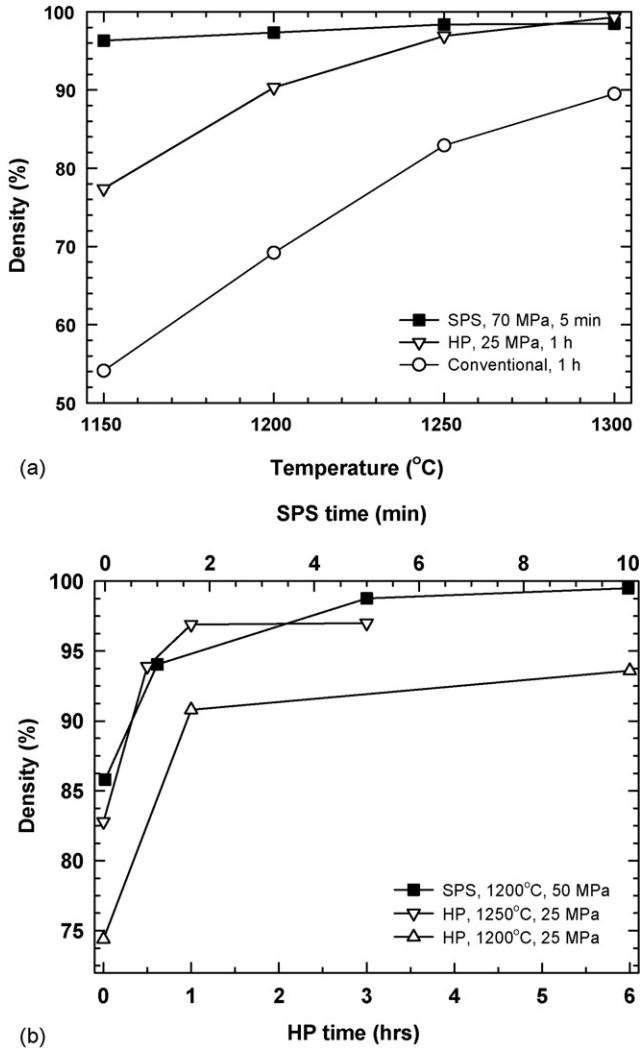

Fig. 2. Densities of YSZ specimens sintered by different techniques at (a) different temperatures and (b) different time.

Fig. 2(b) shows how the density varies with sintering time at constant temperature. SPS shows the highest degree of densification. The density of hot pressed specimen HP-1250-25-1 was measured to 96.9%. In comparison the density of SPS-1200-50-5 was 98.8% showing that both temperature and in particular sintering time can be reduced significantly for the SPS technique compared to HP. An attempt to lower the SPS temperature to 1100 °C by applying a pressure of 110 MPa (SPS-1100-110-8) resulted in a final density of 96.0%. By applying a pressure at the sintering temperature, a final density of 98.5 and 99.3% was obtained for SPS-1150-100-3* and SPS-1150-100-5*, respectively.

3.2. Microstructure and grain growth

FE-SEM micrographs of a selection of sintered YSZ materials are shown in Fig. 3. As seen in Fig. 3(a–d), SPS gives homogenous microstructures with narrow grain size distribution. The grain growth during SPS, with increasing isothermal time at 1200 °C (Fig. 3(a and b)), is moderate compared to the grain growth with increasing sintering temperature (Fig. 3(c and d)). The smallest grain size (0.21 μm) for spark plasma sintered YSZ was obtained for the SPS-1100-110-8 specimen (Fig. 3(c)). In contrast severe grain growth was observed when the SPS sintering temperature was increased from 1100 to 1300 °C (SPS-1300-70-5 shown in Fig. 3(d)). Grain growth during HP with increasing isothermal time at 1250 °C (Fig. 3(e and f)) is moderate, comparable to SPS (Fig. 3(a and b)). The time scale however, is different and specimen HP-1250-25-3 (Fig. 3(f)) showed slightly smaller grains than SPS-1200-50-10 (Fig. 3(b)). The conventionally sintered specimen (CS-1500-12) in Fig. 3(g) has larger grains and with enclosed pores.

The average grain size development for YSZ materials, sintered at different temperatures and times, is displayed in Fig. 4(a and b), respectively. The results indicate that HP is a good technique for densification of YSZ with suppressed grain growth. For relatively dense YSZ (97%), an average grain size

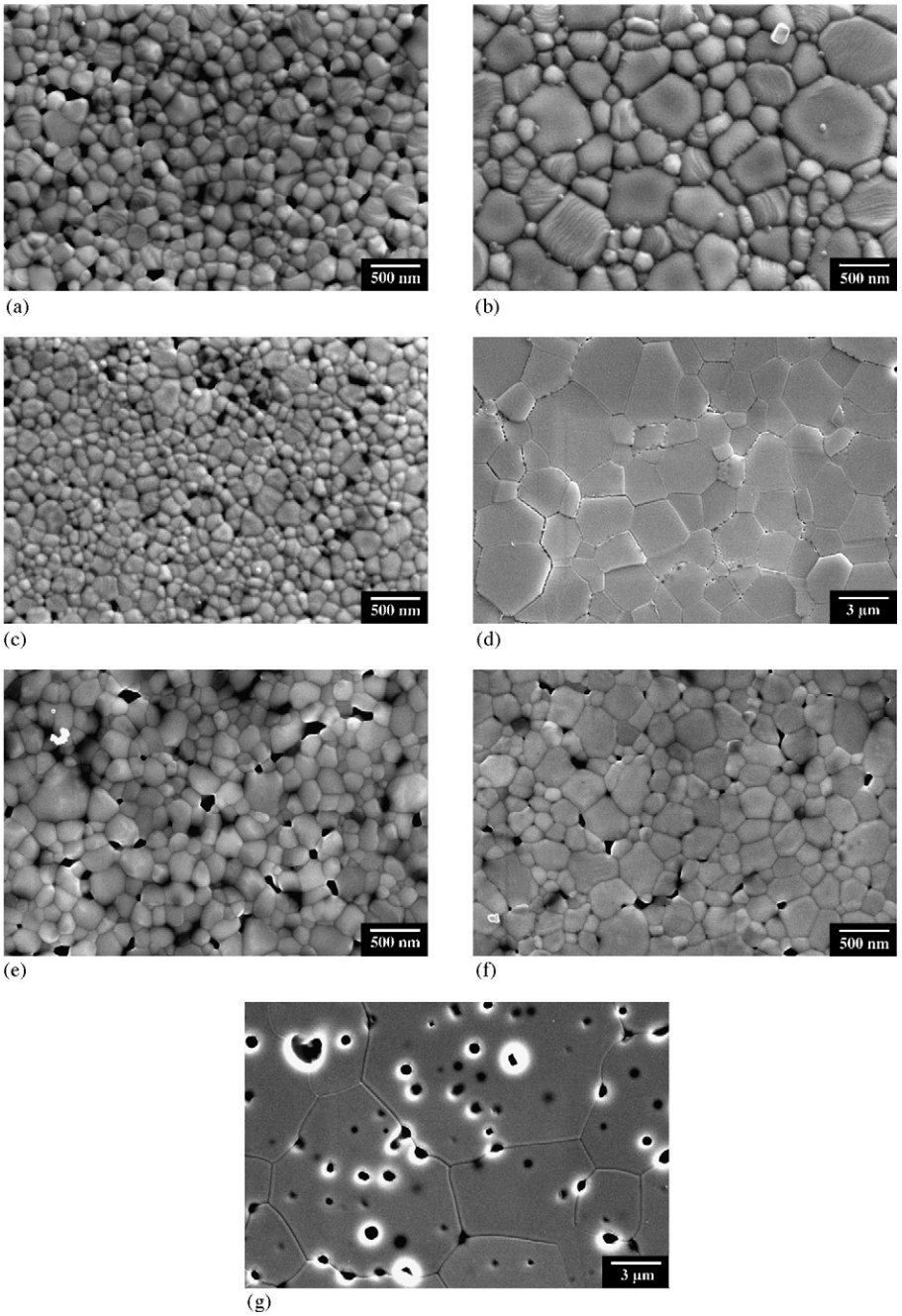

Fig. 3. FESEM micrographs of sintered YSZ specimens after oxidation and thermal etching 50 °C below sintering temperature: (a) SPS-1200-50-0, (b) SPS-1200-50-10, (c) SPS-1100-110-8, (d) SPS-1300-70-5, (e) HP-1250-25-0, (f) HP-1250-25-3 and (g) CS-1500-0-12.

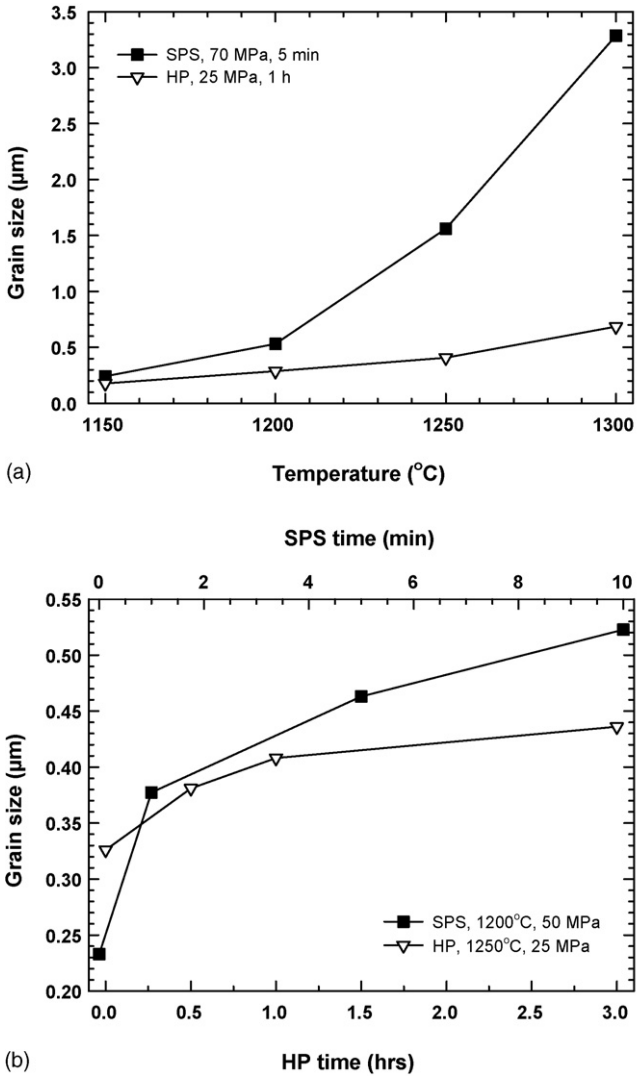

Fig. 4. Average grain size as a function of sintering temperature (a) and time (b) for YSZ sintered by hot pressing and spark plasma sintering (HP: 1 h, 25 MPa, SPS: 5 min, 70 MPa).

down to 0.37 μm was obtained (HP-1250-25-1). The SPS technique shows a more severe grain growth with increasing temperature (Fig. 4(a)) compared to HP, but as a function of time (Fig. 4(b)) the growth is moderate for SPS as well. The average grain size of the conventionally sintered specimen (CS-1500-0-12) was 12 μm.

3.3. Electrical conductivity

The electrical conductivity of selected specimens is presented in Fig. 5 in the form of plots of $\log(\sigma T)$ versus $1000/T$. Table 2 summarizes the electrical conductivity at 900 °C and the associated activation energy for specimens sintered by the different techniques. For YSZ specimens sintered from synthesized powder no clear trend of variation with grain size (varying from 0.21 to 12 μm) was observed for neither conductivity (σ) nor activation energy (E_A). It can however be remarked that E_A for the SPS specimens are in the slightly higher (99–102 kJ/mol) compared to that of the HP

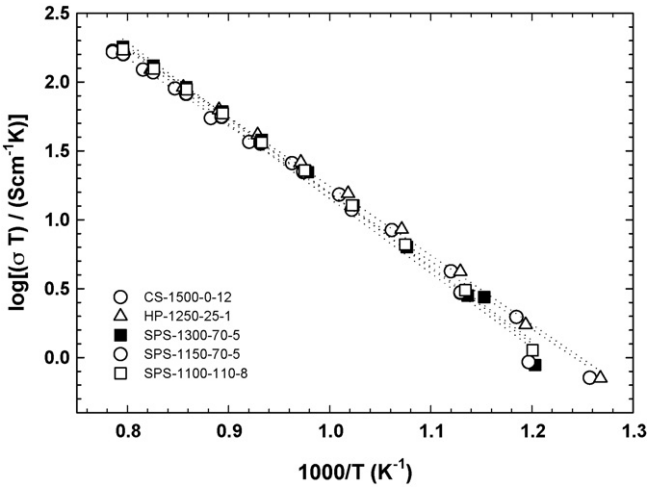

Fig. 5. Logarithmic plot of the electrical conductivity for YSZ materials measured by the van der Pauw technique.

specimen (96 kJ/mol) and conventional sintered specimen (94 kJ/mol).

3.4. Mechanical properties

Vickers hardness (H_V) and fracture toughness (K_{IC}) of YSZ materials with varying grain size are shown in Fig. 6(a and b), respectively. As seen there is no significant change in H_V for specimen with grain size from 0.2 to 12 μm, while the fracture toughness is slightly increasing with decreasing grain size. Fig. 7(a) shows an intergranular crack obtained from a 49 N indent on the SPS-1300-70-5 specimen. Intergranular cracks were observed for all samples except the larger grained conventionally sintered (1500 °C) YSZ specimen which showed intragranular crack behaviour (Fig. 7(b)).

4. Discussion

4.1. Densification

SPS is shown to be a highly efficient technique for densification of YSZ at temperatures 100–200 °C lower than that needed by HP. For HP with an applied pressure of 25 MPa, a temperature of 1300 °C is needed to obtain fully dense (>99% of theoretical value) YSZ materials. In comparison, 1150 °C for 5 min (100 MPa) was sufficient when using the SPS technique. The higher pressure used in SPS can partly explain the lower

Table 2
Properties of YSZ specimens obtained from different sintering techniques

Specimen ID	Density (%)	Average grain size (μm)	Conductivity at 900 °C (mS/cm)	Activation energy (kJ/mol)
CS-1500-0-12	97.5	12	70	94
SPS-1300-70-5	98.5	3.3	83	101
HP-1250-25-1	96.9	0.37	82	96
SPS-1150-70-5	96.3	0.24	75	99
SPS-1100-110-8	96.0	0.21	82	102

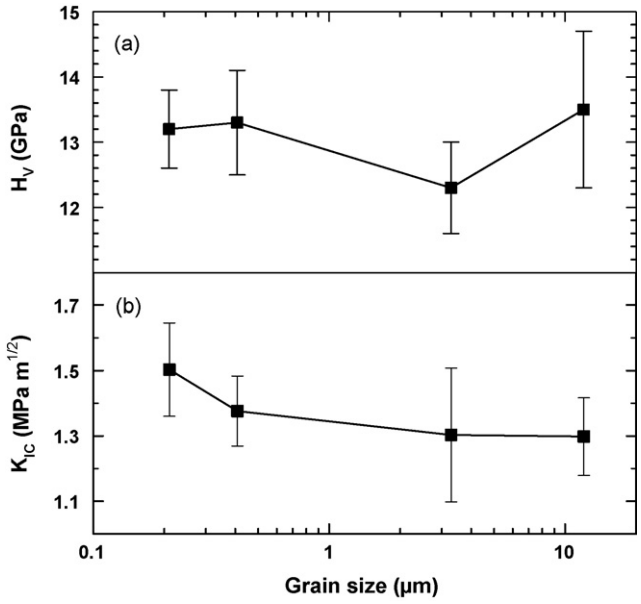

Fig. 6. Vickers hardness (a) and fracture toughness (b) for YSZ materials with different grain size. The uncertainty bars indicate the standard deviations.

sintering temperature. The main reason for both the short sintering time and reduced temperature, however, is the efficient heat transfer as well as the self-heating from spark discharge between the particles. Under these conditions residual carbonates in the powder will be efficiently removed as long as the system is not closed. By not applying the load until the isothermal SPS temperature is reached, CO_2 is allowed to escape the system before the main densification starts. Residual carbonates in the powder have been shown to inhibit the sintering [10]. A more efficient removal of carbonates during SPS compared to HP and conventional sintering can therefore also explain the higher sintering rate and lower sintering temperature. The densification rate by SPS has a maximum 50–100 °C lower than reported by Anselmi-Tamburini et al. for SPS of commercial powder (TZ-8Y) [16].

4.2. Microstructure and grain growth

HP and SPS have been proved to produce dense YSZ materials with small grains compared to conventional

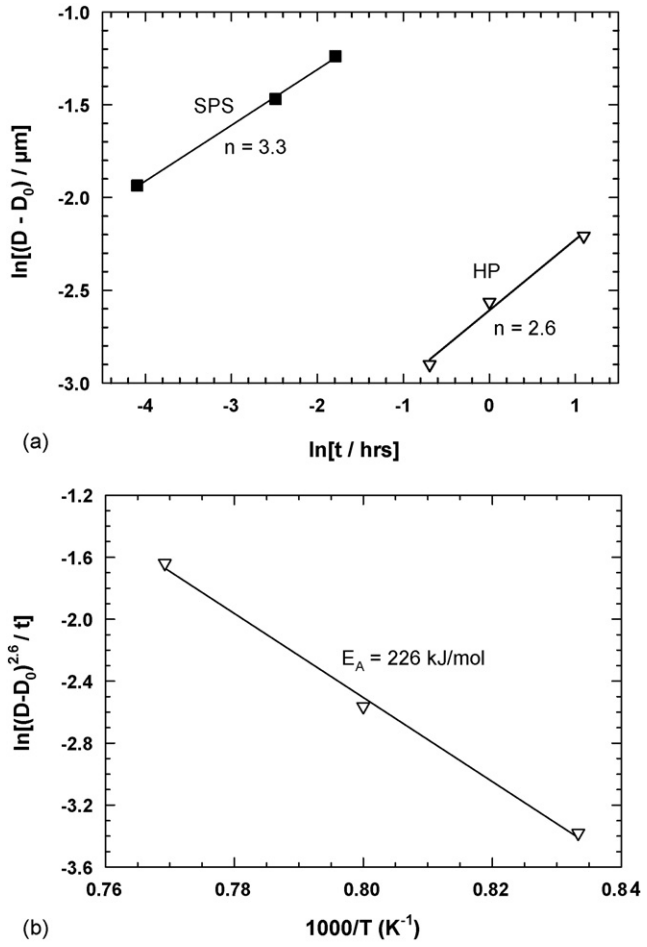

Fig. 8. (a) Grain growth exponents, n, for HP at 1250 °C and SPS at 1200 °C, calculated from the slopes of the linear regression plots of $\ln(D - D_0)$ vs. $\ln(t)$. (b) Activation energy for grain growth during HP, calculated from the slope of the linear regression plot of $\ln((D - D_0)/t)$ vs. $1000/T$.

sintering where severe grain growth is inevitable in the final stage of densification. The kinetics of grain growth during HP and SPS was investigated by calculating the growth order, n and (for HP) the activation energy, E_A, for grain growth. The growth order was calculated from the slope of the linear regression plots shown in Fig. 8(a) assuming the growth obeys a power-law relationship [17]. According to the LSW theory [18,19] the exponent, n, should be equal to 3 when the grain

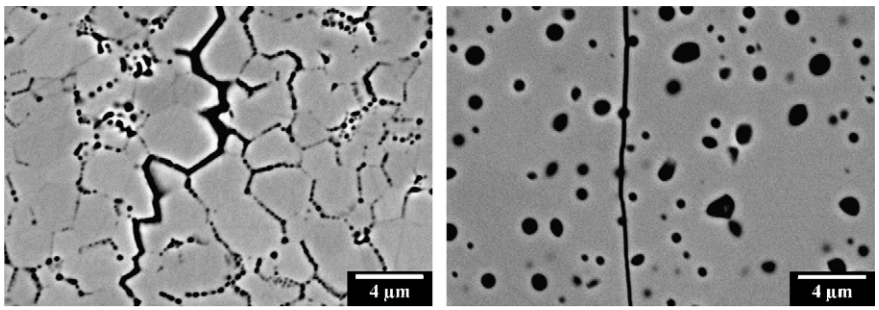

Fig. 7. SEM micrograph of a (a) intergranular crack (from 49 N indent) in YSZ sintered by SPS at 1300 °C (SPS-1300-70-5) and (b) intragranular crack (from 49 N indent) in YSZ sintered conventionally at 1500 °C (CS-1500-0-12).

growth is controlled by volume diffusion. Furthermore, $n = 2$ can be assigned to growth controlled by energy difference across curved interfaces while $n = 4$ is associated with coarsening controlled by grain boundary diffusion. Hence, grain growth for both SPS and HP, with calculated exponents $n = 3.3$ and 2.6, respectively, seem to be dominated by volume diffusion. Even though the exponent n for SPS is higher, the relative grain growth $D - D_0$ is lower for HP. It is shown in Fig. 4(a) how the grain growth for SPS with increasing sintering temperature is far more severe than for HP. More effective decomposition of carbonate species during SPS, giving grain boundaries with higher purity and therefore higher mobility, can explain the higher grain growth rate compared to that of HP.

It should be noted that plotting $\ln(D)$ instead of $\ln(D - D_0)$ as a function of $\ln(t)$ led to unreasonably high growth order values. Simplified plots like this are often reported [20–22] and will for severe grain growth (several orders of magnitude) give satisfactory estimates of n. From our observations we can state that this fails for smaller grain size changes with sintering time. The grain growth observed for SPS follow the same trend as recently reported work on YSZ [16]. The activation energy for grain growth during HP, calculated from the slope in Fig. 8(b), was 226 kJ/mol. This is comparable to reported value of 289 kJ/mol for YSZ (8% Y_2O_3) [23].

4.3. Electrical conductivity

It has been suggested that the difference in conductivity for the polycrystalline specimens from different starting powders could be due to a different level of impurities in the powders. The powder contained a small amount of residual carbonates. However, it is unlikely that carbonates are still present after sintering, particularly by using the SPS technique. At 900 °C, σ varies from 75 to 83 mS/cm and in comparison a total ionic conductivity in the range of 40–60 mS/cm at 900 °C is reported for YSZ (8% Y_2O_3) by Chen et al. [5]. For YSZ (8.7% Y_2O_3) bulk materials with grain size varying from 6.5 down to 1.3 μm, a small variation in electrical conductivity (3–6 mS/cm at 600 °C) has been reported by Tuller [6]. This is comparable to the measured electrical conductivity of 3–5 mS/cm at 600 °C, however in this case no systematic variation with grain size is observed. Calculated activation energies varies from 94 to 102 kJ/mol which is somewhat lower than what is reported by Tuller (111 kJ/mol) [6] and Anselmi-Tamburini et al. (109 kJ/mol) [24]. The colouring of SPS and HP specimens after sintering is an indication of reduced material as previously reported [24]. Increased electronic conductivity would be expected in YSZ specimen containing reduced species acting as charge carriers. Such an effect is not observed as the specimens are oxidized by heating to ∼1000 °C prior to the electrical conductivity measurement. A possible explanation for the higher E_A values for SPS and HP specimens could be carbon impurities from the graphite pressing dies used during sintering. It should be pointed out that no significant weight gain or loss due to oxidation of reduced species or removal of carbon was observed upon heating.

4.4. Mechanical properties

Measured Vickers hardness are in agreement with reported values of 13–15 GPa [15,17,25] and no significant change is observed for different grain sizes. The fracture toughness is somewhat decreasing with increasing grain size. As intergranular fracture is observed, an increase in K_{IC} with increasing grain size should be expected [26]. The observed decrease might be due to the segregation of pores along the grain boundaries, as seen for the SPS specimen in Fig. 7(a). Intergranular fracture in conventionally sintered YSZ (Fig. 7(b)) can be explained by the trapped pores inside individual grains. The intergranular fracture results in lower K_{IC} value compared to the SPS sample sintered at 1100 °C. The obtained K_{IC} values are in agreement with literature values [15,23].

5. Conclusions

In a comparative study of the sintering techniques SPS, HP and conventional sintering, dense YSZ materials (>96% of theoretical), with average grain size of 210 nm, 370 nm and 12 μm, respectively, were obtained by all methods. SPS enables preparation of dense materials with limited grain growth provided appropriate sintering conditions are applied, if not very fast grain growth might occur. No significant differences in electrical conductivity were observed for YSZ materials with grain size varying from 210 nm to 12 μm, however the activation energy for spark plasma sintered material (99–102 kJ/mol) was slightly higher than for HP (96 kJ/mol) and conventional sintering (94 kJ/mol). No clear variation in Vickers hardness was found with varying grain size. The fracture toughness showed a small increase with decreasing grain size.

References

[1] I. Kosacki, T. Suzuki, V. Petrovsky, H.U. Anderson, Solid State Ionics 136–137 (2000) 1225–1233.
[2] I. Kosacki, H.U. Anderson, Ionics 6 (2000) 294–311.
[3] M.C. Martin, M.L. Mecartney, Solid State Ionics 161 (2003) 67–79.
[4] X. Guo, Z. Zhang, Acta Mater. 51 (2003) 2539–2547.
[5] X.J. Chen, K.A. Khor, S.H. Chan, L.G. Yu, Mater. Sci. Eng. A335 (2002) 246–252.
[6] H.L. Tuller, Solid State Ionics 131 (2000) 143–157.
[7] P. Mondal, A. Klein, W. Jaegermann, H. Hahn, Solid State Ionics 118 (1999) 331–339.
[8] C. Petot, M. Filal, A.D. Rizea, K.H. Westmacott, J.Y. Laval, C. Lacour, R. Ollitrault, J. Eur. Ceram. Soc. 18 (1998) 1419–1428.
[9] Z. Shen, M. Johnsson, Z. Zhao, M. Nygren, J. Am. Ceram. Soc. 85 (8) (2002) 1921–1927.
[10] I. Kaus, P. Dahl, J. Mastin, T. Grande, M.-A. Einarsrud, J. Nanomater. (2006) 1–7.
[11] Z. Shen, Z. Zhao, H. Peng, M. Nygren, Nature 417 (2002) 266–269.
[12] M.I. Mendelson, J. Am. Ceram. Soc. 52 (8) (1969) 443–446.
[13] L.J. Van der Pauw, Philips Res. Rep. 13 (1958) 1–9.
[14] G.R. Anstis, P. Chantikul, B.R. Lawn, D.B. Marshall, J. Am. Ceram. Soc. 64 (1981) 533–538.
[15] L. Donzel, S.G. Roberts, J. Eur. Ceram. Soc. 20 (2000) 2457–2462.
[16] U. Anselmi-Tamburini, J.E. Garay, Z.A. Munir, J. Mater. Res. 19 (11) (2004) 3255–3262.

[17] H. Jiang, Y. Lu, W. Huang, X. Li, M. Li, Mater. Charact. 51 (2003) 1–10.
[18] I.M. Lifshitz, V.V. Slyozov, J. Phys. Chem. Solids 19 (1/2) (1961) 35–40.
[19] C. Wagner, ZEITSCHRIFT FUR ELEKTROCHEMIE 65 (1961) 581–591.
[20] S. Tekili, Comp. Sci. Tech. 65 (2005) 967–972.
[21] L. Yang, J.S. Wu, L.T. Zhang, Mater. Des. 25 (2004) 97–102.
[22] T.S. Zhang, J. Ma, Y.J. Leng, Z.M. He, J. Cryst. Growth 274 (2005) 603–611.
[23] S. Tekili, J. Alloy Compd. 391 (2005) 217–224.
[24] U. Anselmi-Tamburini, J.E. Garay, Z.A. Munir, J. Mater. Res. 19 (11) (2004) 3263–3269.
[25] G.A. Gogotsi, S.N. Dub, E.E. Lomonova, B.I. Ozersky, J. Eur. Ceram. Soc. 15 (1995) 405–413.
[26] P.F. Becher, J. Am. Ceram. Soc. 74 (2) (1991) 255–269.